Multi-vehicle Dynamic Pursuit using Underwater Acoustics

Brooks L. Reed, Josh Leighton, Milica Stojanovic and Franz S. Hover

Abstract Marine robots communicating wirelessly is an increasingly attractive means for observing and monitoring in the ocean, but acoustic communication remains a major impediment to real-time control. In this paper we address through experiments the capability of acoustics to sustain highly dynamic, multi-agent missions, in particular range-only pursuit in a challenging shallow-water environment. We present in detail results comparing the tracking performance of three different communication configurations, at operating speeds of $1.5 m/s$. First, when using full-sized modem packets with negligible quantization and a 23-second cycle time, the tracking bandwidth is $0.065 rad/s$. Second, a "lower bound" case with RF wireless communication, a 4-second cycle and no quantization has a tracking bandwidth of $0.5 rad/s$. Third, using 13-bit mini-packets, we employ logarithmic quantization to achieve a cycle time of 12 seconds and a tracking bandwidth of $0.13 rad/s$. These outcomes show definitively that aggressive dynamic control of multi-agent systems underwater is tractable today.

1 Introduction

Marine robots have played an increasing role in ocean operations during recent years, with the proliferation of many commercial platforms and sensors. A major trend is toward tetherless operations, for which each vehicle has to carry its own power source and have a means of wireless communication. Over distances beyond

---

Brooks Reed
MIT/WHOI Joint Program in Oceanographic Engineering, e-mail: brooksr8@mit.edu

Josh Leighton, Franz Hover
Massachusetts Institute of Technology, 77 Massachusetts Ave., Cambridge MA 02139,
e-mail: jleight@mit.edu, hover@mit.edu

Milica Stojanovic
Northeastern University, 360 Huntington Ave., Boston, MA 02115
e-mail: millitsa@ece.neu.edu

about one hundred meters, underwater communication is almost exclusively accomplished through acoustics, and the wireless nature of this channel lends itself naturally to multiple agents. Acoustic communications bring many challenges, however, such as packet loss, low data rates, and delays; Heidemann *et al.* provide a recent review [23]. These undesirable properties of acoustic communications have limited its use in high-performance, real-time tasks. Typical experiments with acoustic modems address packet loss rates between vehicles [7, 9], distributed navigation [1], and communication of commands or data between vehicles and ships [29].

If a capability existed, truly dynamic missions of interest would include networked ocean vehicles following a submarine or a marine animal; the latter has been a dream of biologists for decades. Major gaps exist in our understanding of the life cycles of many important marine animals, such as jellyfish [28], sharks [31, 36], lobsters [34], and more. Dynamic pursuit with marine vehicles and appropriate sensors can help give biologists the data they need to fill in these gaps. A broader and more challenging problem is monitoring and following a quickly-evolving plume or other oceanic process [8, 18], where distributed measurements become critical for assimilation with models and subsequent adaptive sampling [25]. These tasks involve *dynamic feedback control that relies explicitly on acoustic communication*, and fit into the growing field of network-based control [2]. In an effort to lay some groundwork for exploiting advanced algorithms in a real-world ocean application, this paper addresses with experiments an approach for joint estimation and pursuit of a moving target using acoustic communications; see **Figure 1**. Needless to say,

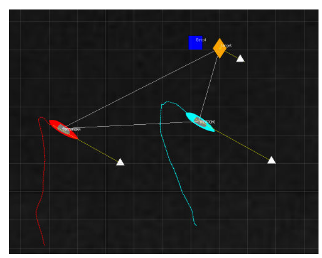

Fig. 1 Screenshot from Team Underwater Localization and Pursuit (TULiP) experiment with acoustic communications. The two vehicles jointly estimate the target location based on range measurements, and move to stay in formation relative to it.

the general pursuit problem has held high interest for decades; it is a canonical mission in space and air, on land, and at sea. Probabilistic pursuit-evasion games have been studied extensively in the robotics literature [35], and pursuer and evader dynamics as well as nonlinear estimation are important factors in these algorithms [26, 37]. However, the effects of communication constraints have not received much attention [27]. These are often addressed indirectly via decentralized approaches that require minimal exchange of information between agents [11]; see [21, 16] for ocean-specific implementations.

There have also been, however, some recent experimental works that are related to our pursuit scenario. Perhaps most intriguing is tracking a leopard shark in extremely shallow water, using a single autonomous vehicle with a hydrophone array of 2.4*m* spread [12]. The system was successful but the shark evidently moved only 200*m* or so in 48 minutes reported. Bean *et al.* (2007) studied range-based leader–

follower regulation with MicroModem mini-packets with $1m/s$ speeds [3], while Brignone *et al.* (2009) study a similar problem with DSPComm modems and two vehicles operating at 0.7 and $3m/s$ [6]. Both works present data from proof-of-concept field trials with mostly straight trajectories. Soares *et al.* (2013) consider a vehicle following two leaders in a triangle formation, with ranges of about fifteen meters, speeds around $0.5m/s$, and a total loop time of four seconds [32]. In contrast, Cruz *et al.* (2012) consider a complete feedback system—in the sense of two-way communications—for which a stationary controller transmits commands for two mobile followers, who then transmit back their positions [13]. The vehicle speeds are slow, in the neighborhood of $10cm/s$, and the cycle time is around twenty seconds. Through analysis, Chen and Pompili (2012) addressed optimization of the special considerations of acoustic communications in coordinated flight of ocean gliders, where currents are especially important [10].

None of these prior works explicitly deal with designing and improving closed-loop frequency response of an integrated multi-vehicle feedback system. This is exactly our objective here. Our design does not rigorously account for stability margins, the multi-rate nature of acoustic communications, inherent geometric nonlinearities, or the fact that automous marine vehicles are not ideal actuators. On the other hand, our approach clearly demonstrates practical closed-loop performance at half the Nyquist rate, with little evidence of stability breakdown.

We detail the experiment setup in the following section with descriptions of the vehicles and communication hardware used, the experimental domain, and the estimation and control strategies and parameters. We then give results from three integrated tests, demonstrating the performance achieved.

2 Experimental Setup

Our experiment, **T**eam **U**nderwater **L**ocal**i**zation and **P**ursuit (TULiP), has two mobile agents sharing range information and commands through acoustic links. We make scalar range measurements at each agent, and thus tracking is impossible without their coordination. One agent is designated as the leader that coordinates the measurements and the actions of one or more followers. This arrangement involves lossy channels at both locations in the feedback loop of **Figure 2**. In the general case, a centralized architecture such as this allows integration with remote sensing, large-scale computations (such as data assimilation), and human-in-the-loop decision-making. The mobile agents attempt to stay close to the target, and in a formation conducive to good sensor performance. For our pursuit scenario, a distributed mobile array that utilizes range measurements offers benefits of simpler sensors, more maneuverable vehicles, and increased flexibility compared to systems relying on bearing measurements. However, even when directional or gradient information is available at a single agent, e.g. through a towed array of hydrophones or sensors, exploiting multiple vehicles should give substantial improvements.

The next five subsections detail the arrangement and operation of this complex system.

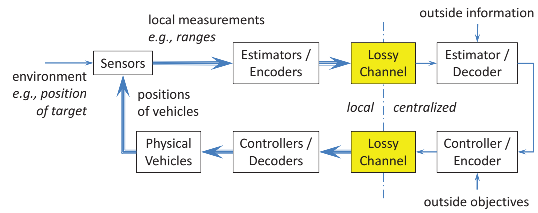

Fig. 2 Block diagram of a generic multi-vehicle feedback system with a centralized estimator and controller, and communication channels in two locations in the loop. Vehicles act as mobile sensors.

2.1 Autonomous Surface Vehicles

We use autonomous kayaks as shown in **Figure 3** for our experiments; they are also described in [22]. Each craft is $1.8m$ long, weighs about $40kg$, and has a rotating thruster near the bow for propulsion and steering. In these tests, the vehicles operate at a nominal speed of $V = 1.5m/s$. The relevant navigation sensors available on each vehicle are a tilt-compensated compass and RTK GPS. We use Novotel GPS antennas, uBlox GPS receivers, and the RTKlib software package [33]. With a fixed base station on shore and communications over wifi, we have observed GPS position variances on the order of $10^{-4}m^2$. Raw compass measurements are passed through a first-order low-pass filter with time constant $1.95s$, and the noise variance on this signal is estimated as $10deg^2$.

The vehicles run MOOS-IvP autonomy software [4] integrated with custom control algorithms and modem interfaces. We rely on the the MOOS heading PID controller, which runs at five Hz, and the MOOS trackline controller, which runs at two Hz. Step response experiments with the kayak under closed-loop heading control indicate a rise time of roughly four seconds, and 30% overshoot; we also note the kayaks are able to turn 180 degrees in approximately three seconds. The MOOS trackline controller is an inner-outer loop that modulates the desired vehicle heading so as to steer it toward a point on the trackline, some lead distance l_d ahead. When the waypoint is closer than the lead distance, the vehicle simply drives towards the waypoint. For longer distances the result for small errors is a proportional map for desired heading: $\phi^d \simeq e_x/l_d$, where e_x is the cross-track error in meters and ϕ^d is in radians.[1] We set $l_d = 15m$ for these experiments.

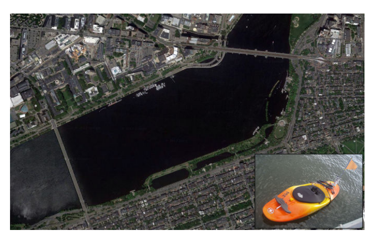

Fig. 3 The Charles River Basin in Cambridge/Boston, MA, and the autonomous kayak Nostromo. Water depth is 2-12m.

[1] The linear form written is based on approximation of the tangent function. For errors less than one meter, the MOOS Trackline controller increases the lead distance proportionally, effectively lowering the gain to limit oscillations.

2.2 Acoustic Communications

We use the the WHOI Micro-Modem [19], a well-established and commercially available technology for underwater acoustic communication. Modems are towed by the vehicles, suspended at a depth of about 1.5 meters; this gives us realistic shallow-water acoustic performance, but with direct access to GPS and RF wireless connectivity at the surface for conducting controlled tests. Along with messaging, we use the modem for one-way travel-time ranging [17]. The WHOI MicroModem has six different packet types with different lengths and data capacities. In this work, we use the FSK mini-packet ("MP"), which is regarded as the most robust of the packet types, but contains only thirteen bits of information. Nominally, the mini-packets take slightly over one second to transmit. We also use the full-sized Rate 0 FSK packets ("FSK0"), which carry thirty-two bytes of information and nominally take five seconds to transmit. We have observed very large increases in packet loss when using small guard times with both packets, and have found communications to be most reliable with four-second slots for mini-packets and 9.5-second slots for FSK0 packets. All MicroModem packets are sent with an acoustic source level of 190 dB rel μPa.

The Charles River Basin has fresh water 2-12*m* deep, a complex bathymetry, and some hard surfaces on the boundaries (seawalls and bridges); our working space is about 1500*m* long and 500*m* wide. Acoustic performance in this environment is different from an open-water deep ocean scenario, where multipath and reverberation are much lower, but the ranges are higher. Operations in the Basin can have highly variable acoustic performance, as shown in **Figure 4**. Our conditions are multipath-limited and travel times are short.

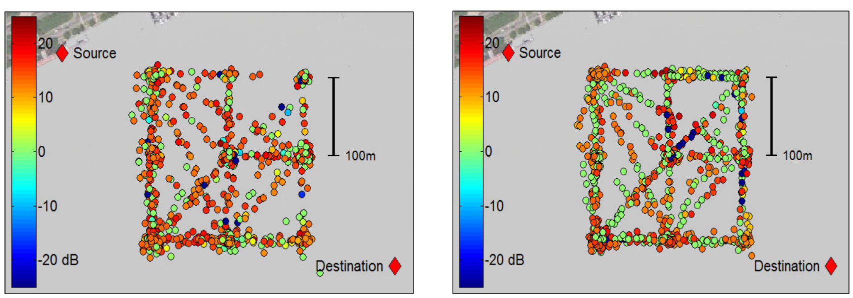

Fig. 4 Micro-Modem performance data in the Charles River Basin, an environment limited by multipath, not power. The left plot shows transmissions from the source to a mobile relay, and the right plot shows transmissions from the relay to the destination. The SNR value indicates sound pressure level relative to ambient noise.

2.3 TULiP Physical Layout

The two-vehicle pursuit mission encompasses limited communication performance in both the sensing and control channels. In this experiment there is a target to be tracked, "Icarus", and two cooperating agents "Silvana" and "Nostromo". We will denote these three nodes with the symbols $\mathcal{I}$, $\mathcal{S}$, and $\mathcal{N}$, respectively. $\mathcal{N}$ can be thought of as a leader, and $\mathcal{S}$ a follower; our basic approach extends easily to multiple followers. The sensing objective is a simple one: to maintain $\mathcal{S}$ and $\mathcal{N}$ in fixed triangular configuration relative to the estimated location of $\mathcal{I}$, so that measurements will be of high fidelity, *i.e.*, in the sense of a good HDOP [5], and in the sense of a short range. Our pursuit arrangement models the general situation where range or other target sensing degrades with distance, but a high level of tracking precision is desired. Maintaining a close pursuit formation keeps ranges near a nominal value with small perturbations, allowing for more precise quantization as discussed in the following section. Practically, our modems have plenty of power but a small formation allows us to effectively study the dynamic effects of closed-loop pursuit.

However, an "unstable" situation is encountered if the target crosses the baseline (the line in between the two vehicles acting as a moving long baseline network); when this occurs the estimate begins to diverge from the target location. The disadvantage of a small pursuit formation is that it is easier for the target to cross the baseline, bringing up a tradeoff between robustness of a larger formation and accuracy of a smaller formation. Closed-loop performance must be high for the accuracy of the smaller formation to be realized.

2.4 Cycle Description, Timing and Quantization

We detail the stages of the control loop for the MP and FSK0 cases. Within a cycle step, $\mathcal{S}$ and $\mathcal{N}$ each receive a measurement of range to $\mathcal{I}$ via the Micro-Modems in ranging mode. After a guard period, $\mathcal{S}$ transmits its current location and range data to $\mathcal{N}$ through acoustic communication. $\mathcal{N}$ combines this information with its own location and range information to generate an estimated location of $\mathcal{I}$. $\mathcal{N}$ calculates control actions for itself and for $\mathcal{S}$, and transmits the latter back to $\mathcal{S}$. The cycle includes three separate transmissions and there are no acknowledgments. We enforce the fixed time slots with a number of timeouts, as indicated in **Figure 5**. We synchronize clocks using the network time protocol; in the absence of clock synchronization, we note that precision clocks are becoming increasingly practical for use on underwater vehicles [17].

For feedback control, there is a problem-dependent tradeoff to be made between time-averaged throughput (usually achieved with long coding blocks) and timeliness of the information (shorter messages). We present data using both 13-bit minipackets and 32-byte FSK0 packets as an initial study of this tradeoff. The MP scenario minimizes cycle time at the expense of data quantization; we achieved a total

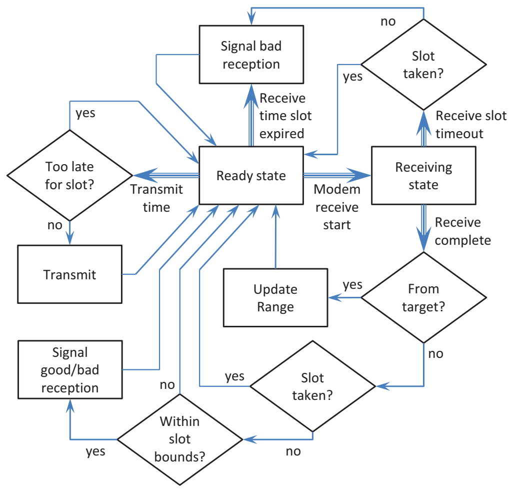

Fig. 5 The internal state machine used on each vehicle in the TULiP mission to maintain consistent timing with respect to predefined transmission and reception slots. Thick arrows distinguish acoustic events that initiate state changes or other actions from normal logic flow. Special operations are indicated to handle detection of erroneous multipath receptions, which frequently occur in this environment. For example, a good reception for a time slot T_i will follow the "Receive complete" path (bottom) to a good signal. A trailing multipath reception will return to the receiving state, but the end of time slot T_i will arrive before the end of the packet. In the top right, slot T_i is already taken by the good reception, so we return to the ready state with no action taken.

cycle time of 12 seconds in this configuration.[2] With the FSK0 configuration, packets require no quantization for the data types we send, however require a 9.5*sec* time slot for each transmission, resulting in a total cycle time of 23 seconds.[3] The "wifi" scenario involves a four second slot for acoustic ranging, as detailed above. However, the inter-vehicle communications are handled instantaneously via wifi, so the estimate is available immediately upon reception of ranges.

For the message from $\mathcal{S}$ to $\mathcal{N}$ in the MP case, we used three bits for the range, and five bits each direction for $\mathcal{S}$'s location in a 32×32 discretized workspace; this workspace had ten-meter resolution. The range data were logarithmically quantized relative to a desired range of $50m$, with seven bin edges located at [19.2 32.5 42.5 50 57.5 67.5 80.8]m, and the three-bit messages decoded as [11.5 26.8 38.2 46.8 53.2 61.8 73.2 88.5]m. This correlates with the density $\rho = 0.75$ [20]. For the message from $\mathcal{N}$ back to $\mathcal{S}$, we used five bits in x and y for the desired location in the workspace. This left three bits unused. Note that with quantization, there is a tradeoff between range and precision. With this choice, any range larger than $80.8m$ is

---

[2] When range measurements do not interfere with modem packets and the cycle consists of just two-way communications (*e.g.* using GPS and wifi for ranges), we have achieved a six-second total cycle time with mini-packets in the field.

[3] As we were submitting this paper we became aware of several modifications in the operation of the MicroModems that likely will allow for slightly faster cycle times.

decoded as the furthest range bin, so when ranges are very large, estimation suffers. Increasing this outer range would come at the expense of resolution of the bins near the $50m$ nominal range; it is the control system's job to keep the vehicles in the desired formation so that small bins can be used.

2.5 Settings and User Choices

The tracking system contains a nonlinear sigma-point filter (SPF) [24], well-suited for this type of application.[4] The nonholonomic target is assumed to be moving at constant speed in the plane of $1.55m/s$, with stochastic low-pass, zero-mean turning rate with variance Q. These values are set to be consistent with the motion of the small motorboat that was $\mathcal{T}$. The observation vector contains the two noisy ranges, with variances R_S and R_N for range measurements to Silvana and Nostromo, respectively. The sensor noise for range measurements was chosen based on prior characterizations of the WHOI MicroModem ranging capability [19, 14] and our own observed LBL performance. The sensor noise for the follower range measurement ($\mathcal{T}$ to $\mathcal{S}$) in the MP experiment was set to a higher value to account for the effects of quantization during communication of the measurement from $\mathcal{S}$ to the filter running on $\mathcal{N}$. Settings for the three configurations are given in **Table 1**.

When a measurement is not available (either due to a missed LBL range, or a dropped measurement packet from $\mathcal{S}$ to $\mathcal{N}$), we take the standard approach of setting the noise of the lost measurement to infinity [30]. In the MP and FSK0 configurations, when a control command from $\mathcal{N}$ to $\mathcal{S}$ is dropped, the previously-received command for $\mathcal{S}$ remains the desired waypoint. This approach is chosen to ensure safe operation in the case of many missed packets. In the MP case, three bits are left unused in the command packet which could encode contingency plans.

The desired observation triangle has a sixty-degree vertex at $\mathcal{T}$. For the MP and wifi cases, the ranges to each of $\mathcal{S}$ and $\mathcal{N}$ were $50m$; for the FSK0 case the ranges were $100m$ due to the slower cycle time.[5]

Table 1 Settings and results for the three configurations. Des. Range is the length of the legs in the desired sensing formation. The columns with R are the sensor noise variance for the range measurements to each vehicle. Q is the target heading rate variance. BW is the closed-loop tracking bandwidth, and Atten. is the tracking error attenuation at $0.065 rad/s$.

Config	Cycle Time *sec*	Des. Range *m*	R_S m^2	R_N m^2	Q $(rad/s)^2$	BW rad/s	Atten dB
FSK0	23	100	0.25	0.25	0.01	0.065	0
Wifi	4	50	0.25	0.25	0.05	0.5	18
MP	12	50	0.25	9	0.05	0.13	7

[4] Other nonlinear, range-only filters, such as particle filters, could also be used [15].

[5] The ranges are set relative to the distance the target can drive in a time step, so that the target is unlikely to cross the baseline before the control system can react.

3 Experimental Results

We compare the tracking performance of three different communication configurations. First, we use full-sized Rate 0 frequency-shift-keyed packets ("FSK0") with negligible quantization and a 23-second cycle. Second, we study the case where the two vehicles communicate with RF wireless communication ("wifi"), a 4-second cycle and no quantization. This configuration roughly represents a single vehicle towing a large array, as inter-vehicle communication is lossless and immediate. Third, we use the 13-bit mini-packet ("MP") and employ logarithmic quantization to achieve a cycle time of 12 seconds.

The experiments we report were conducted on 8-9 July 2013, both days with light winds.[6] **Figures 6, 7, 8** give results from the FSK0, wifi and MP tests, respectively. In each test, $\mathcal{T}$ moved in a largely random trajectory, as shown in the birds-eye view in the upper left of the plots (Subplot **a**) and the time traces in Subplot **c**. The upper right (Subplot **b**) shows the sensing formation every fifteen time steps; we see that while the ideal triangle configuration was rarely achieved in the FSK0 and MP tests, the target did not cross the baseline (the red straight line between the two nodes acting as a moving LBL network), nor did the geometry ever stay poor for a sustained period. The tracking and pursuit system did not lose the target.

The measured ranges are reported in the lower subplot in each figure, including quantization of raw values sent to $\mathcal{N}$ from $\mathcal{S}$ in the subsequent measurement packet for the MP case. Range losses in all cases are low, as the MicroModem ranging ping is fairly robust; see figure captions for loss statistics. Subplot **d** shows the north and east tracking error over time, along with dropped communication packets for the mini and FSK cases. The packet losses are significantly higher for the FSK0 test, dramatically illustrating the tradeoff between packet types and packet loss. Most of the larger errors occur following packet losses, however some large spikes (such as around 500 seconds in the mini-packet test) are not near packet losses—errors can also occur due to poor sensing geometry, and in the MP case, quantization.

Recalling our broad objective to achieve dynamic control through mobile acoustic networks, it is revealing to ask what is the effective closed-loop estimation bandwidth achieved. A direct FFT-based empirical transfer function for the estimation error divided by target motion is shown for each test in **Figure 9**; spectra have been smoothed with a 5-point centered moving average. The FSK0 test has a break frequency for tracking the motion of $\mathcal{T}$ of approximately $0.065 rad/s$, slightly less than half the Nyquist rate for the twenty-three-second cycle. The wifi test has a break frequency of approximately $0.5 rad/s$, over half the Nyquist rate for this cycle time of four seconds. The MP test has a break frequency of approximately $0.13 rad/s$, about half the Nyquist rate for the twelve-second cycle. We can also compare the attenuation of tracking error for each configuration at $0.06 rad/s$. FSK0 has zero attenuation, wifi has 18 dB attenuation, and MP has 7 dB attenuation. These results are summarized in **Table 1**.

[6] This data, along with videos, is publicly available at `http://web.mit.edu/hovergroup/resources.html`.

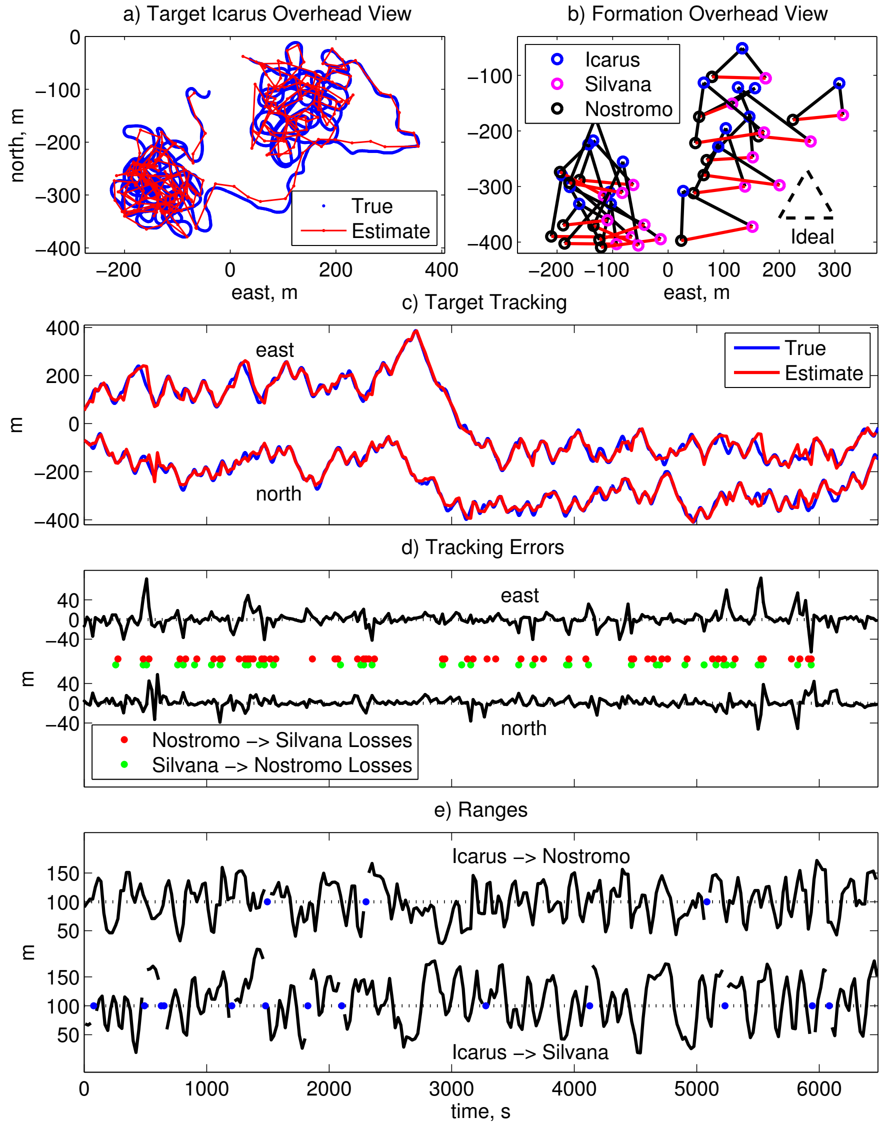

Fig. 6 FSK0 test results (6463 seconds, 281 cycles). a) Overview of the true and estimated trajectories of the target Icarus. b) Sensing formation every 15 time steps. c) Actual (GPS) and estimated trajectory of the target Icarus. d) Estimation error of Icarus' location. The RMS radius of estimation errors was $20.2m$. Data packet losses are also shown; the loss rates were: $\mathcal{N} \rightarrow \mathcal{S} = 19.9\%$, $\mathcal{S} \rightarrow \mathcal{N} = 14.0\%$. e) Range measurements from Icarus to each vehicle, and losses. Range loss rates were: $\mathcal{I} \rightarrow \mathcal{N} = 1.1\%$, $\mathcal{I} \rightarrow \mathcal{S} = 4.8\%$.

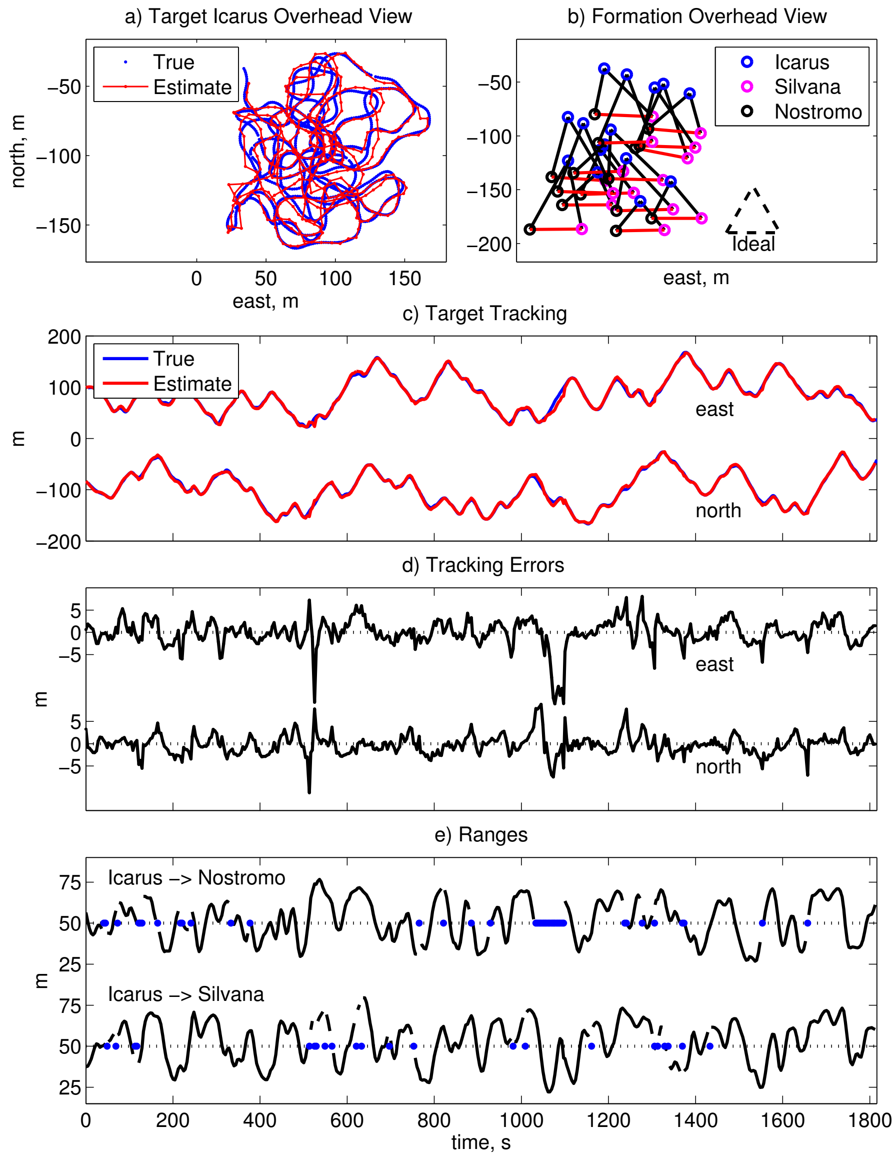

Fig. 7 Wifi test results (1820 seconds, 455 cycles). a) Overview of the true and estimated trajectories of the target Icarus. b) Sensing formation every 30 time steps. c) Actual (GPS) and estimated trajectory of the target Icarus. d) Estimation error of Icarus' location. The RMS radius of estimation errors was 3.8*m*. e) Range measurements from Icarus to each vehicle, and losses. Range loss rates were: $\mathcal{I} \to \mathcal{N} = 9.0\%$, $\mathcal{I} \to \mathcal{S} = 4.8\%$.

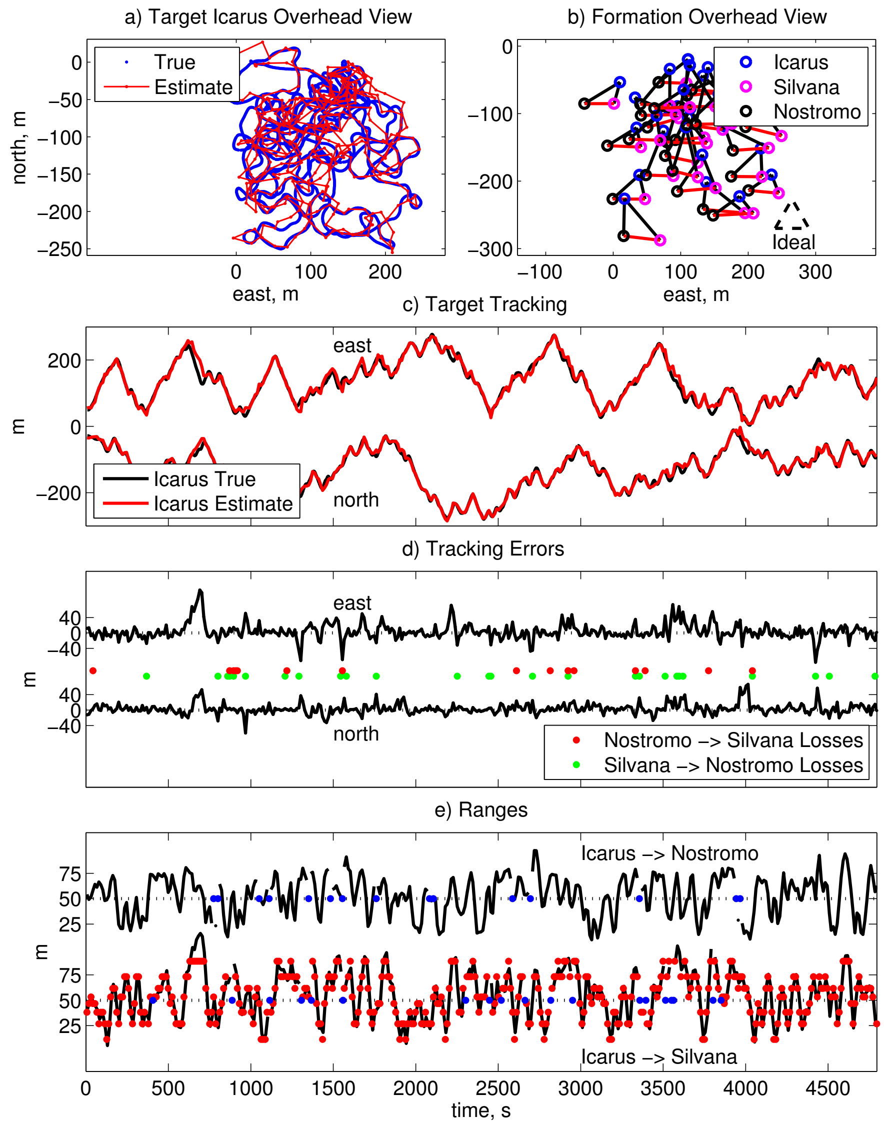

Fig. 8 MP test results (4800 seconds, 400 cycles). a) Overview of the true and estimated trajectories of the target Icarus. b) Sensing formation every 15 time steps. c) Actual (GPS) and estimated trajectory of the target Icarus. d) Estimation error of Icarus' location. The RMS radius of estimation errors was $12.7m$. Data packet losses are also shown; the loss rates were: $\mathcal{N} \rightarrow \mathcal{S} = 3.8\%$, $\mathcal{S} \rightarrow \mathcal{N} = 6.5\%$. e) Range measurements from Icarus to each vehicle, and losses. Range loss rates were: $\mathcal{I} \rightarrow \mathcal{N} = 3.8\%$, $\mathcal{I} \rightarrow \mathcal{S} = 4.8\%$. Quantized measurements sent from Silvana to Nostromo are shown in red on top of the true measured ranges.

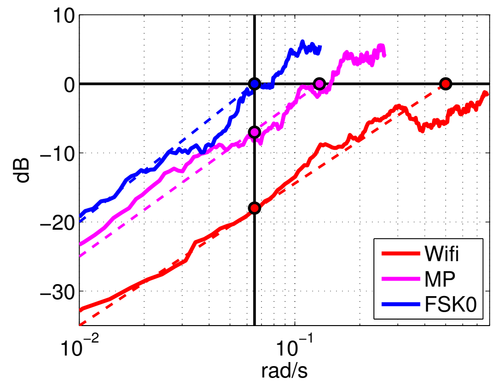

Fig. 9 Empirical FFT-based transfer function for estimator error divided by target motion. The solid lines show the mean of the X and Y spectra. The dashed lines show an approximate linear fit for low-frequency attenuation. Dots show the approximate bandwidth and attenuation at $0.065 rad/s$. Note that due to different cycle times, the Nyquist rate for each experiment is different.

On top of longer cycle times, the mini-packet and FSK0 cases are affected by communication packet losses, and the mini-packets also by quantization, so the degradation in performance compared to wifi is expected. We note that the surface vehicles we use (and underwater vehicles without arrays) are highly maneuverable; a true “single-vehicle with array” configuration would be subject to much more stringent maneuverability constraints and could not pursue the target as closely without risking the target crossing the baseline. For close pursuit, we can view the wifi case as a lower bound on performance achievable with realistic communications. The FSK0 and mini-packet results suggest that if tracking bandwidth is desired, it is advantageous to reduce the cycle times as much as possible, even at the expense of extreme quantization.

4 Conclusion

Our TULiP experiment has achieved aggressive target pursuit in the underwater environment. As opposed to a traditional control and estimation design scenario, the mission here is accomplished through a highly integrated vehicle system performing full joint estimation and coordination through lossy acoustic communications underwater. The three experimental configurations studied show the effects of cycle time, quantization, and acomms performance on the frequency response of the system. In particular, the MP and FSK0 experiments demonstrate that for tracking highly dynamic targets it is beneficial to trade-off quantization for low cycle time.

More broadly, the pursuit mission presented in this paper is a special case of a much larger picture we envision for the future. Undersea communications and coordinated control will enable truly distributed and dynamic tracking of moving ocean features, such as eddies, plumes and fronts. Such vehicle systems would be able to observe important chemical, biological, and physical processes over larger physical scales than a single vehicle can cover, and would interface with observation systems on land and in the atmosphere, as well as humans. Operations like this –

"oceanographic pursuit" – are a natural progression of marine technology toward the group autonomy and dynamic behavior that we have seen developed already in the terrestrial environment and in the air. In such systems, specification of physical configurations, scheduling, routing, and multi-rate control design will undoubtedly join the mix, making underwater pursuit a rich problem for future work.

Acknowledgements Work is supported by the Office of Naval Research, Grant N00014-09-1-0700, the National Science Foundation, Contract CNS-1212597, and the Finmeccanica Career Development Professorship. We thank Mei Cheung for providing Figure 4 and help with experimental implementation. We thank Toby Schneider and Mike Benjamin at MIT, and Keenan Ball and Sandipa Singh at WHOI, for their terrific help on technical items. We also acknowledge MIT Sailing Master Fran Charles.

References

[1] Bahr, A., Leonard, J., Fallon, M.: Cooperative localization for autonomous underwater vehicles. International J. Robotics Research **28**(6), 714 (2009)
[2] Baillieul, J., Antsaklis, P.: Control and communication challenges in networked real-time systems. Proc. of the IEEE **95**(1), 9–28 (2007)
[3] Bean, T., Canning, J., Beidler, G., O'Rourke, M., Edwards, D.: Designing and implementing collaborative behaviors for autonomous underwater vehicles. In: Proc. International Symposium on Unmanned Untethered SubmersibleTechnology (2007)
[4] Benjamin, M., Leonard, J., Schmidt, H., Newman, P.: An overview of MOOS-IvP and a brief users guide to the IvP helm autonomy software. Massachusetts Institute of Technology, MIT CSAIL, Tech. Rep. TR-2009-28-07 (2009)
[5] Bingham, B.: Predicting the navigation performance of underwater vehicles. In: Proc. IEEE/RSJ Intelligent Robots and Systems, 2009 (2009)
[6] Brignone, L., Alves, J., Opderbecke, J.: GREX sea trials: first experiences in multiple underwater vehicle coordination based on acoustic communication. In: Proc. MTS/IEEE OCEANS (2009)
[7] Caiti, A., Calabro, V., Dini, G., Duca, A., Munafo, A.: AUVs as mobile nodes in acoustic communication networks: Field experience at the UAN10 experiments. In: Proc. MTS/IEEE OCEANS (2011)
[8] Camilli, R., Reddy, C., Yoerger, D., Van Mooy, B., Jakuba, M., Kinsey, J., McIntyre, C., Sylva, S., Maloney, J.: Tracking hydrocarbon plume transport and biodegradation at Deepwater Horizon. Science **330**(6001), 201 (2010)
[9] Canning, J., Anderson, M., Edwards, D., O'Rourke, M., Bean, T., Pentzer, J., Odell, D.: A low bandwidth acoustic communication strategy for supporting collaborative behaviors in a fleet of autonomous underwater vehicles. US Navy J. Underwater Acoustics (2009)
[10] Chen, B., Pompili, D.: Team formation and steering algorithms for underwater gliders using acoustic communications. Computer Communications **35**(9), 1017–1028 (2012)

[11] Chung, T., Burdick, J., Murray, R.: A decentralized motion coordination strategy for dynamic target tracking. In: Proc. IEEE International Conference on Robotics and Automation, pp. 2416 –2422 (2006)

[12] Clark, C.M., Forney, C., Manii, E., Shinzaki, D., Gage, C., Farris, M., Lowe, C.G., Moline, M.: Tracking and following a tagged leopard shark with an autonomous underwater vehicle. Journal of Field Robotics **30 (3)**, 309–322 (2013)

[13] Cruz, N.A., Ferreira, B.M., Matos, A.C., Petrioli, C., Petroccia, R., Spaccini, D.: Implementation of an underwater acoustic network using multiple heterogeneous vehicles. In: Proc. MTS/IEEE Oceans, pp. 1–10. IEEE (2012)

[14] Curcio, J., Leonard, J., Vaganay, J., Patrikalakis, A., Bahr, A., Battle, D., Schmidt, H., Grund, M.: Experiments in moving baseline navigation using autonomous surface craft. In: Proc. MTS/IEEE OCEANS (2005)

[15] Dellaert, F., Fox, D., Burgard, W., Thrun, S.: Monte carlo localization for mobile robots. In: Robotics and Automation, 1999. Proceedings. 1999 IEEE International Conference on, vol. 2, pp. 1322–1328. IEEE (1999)

[16] Eickstedt, D., Benjamin, M., Schmidt, H., Leonard, J.: Adaptive tracking of underwater targets with autonomous sensor networks. US Navy J. Underwater Acoustics **56**, 465–495 (2006)

[17] Eustice, R.M., Singh, H., Whitcomb, L.L.: Synchronous-clock one-way-travel-time acoustic navigation for underwater vehicles. J. Field Robotics, Special Issue on State of the Art in Maritime Autonomous Surface and Underwater Vehicles **28**(1), 121–136 (2011)

[18] Farrell, J., Pang, S., Li, W., Arrieta, R.: Chemical plume tracing experimental results with a REMUS AUV. In: Proc. MTS/IEEE OCEANS, vol. 2, pp. 962–968. IEEE (2003)

[19] Freitag, L., Grund, M., Singh, S., Partan, J., Koski, P., Ball, K.: The WHOI micro-modem: an acoustic communications and navigation system for multiple platforms. In: Proc. MTS/IEEE OCEANS (2005)

[20] Fu, M., Xie, L.: The sector bound approach to quantized feedback control. IEEE Trans. Automatic Control **50**(11), 1698 – 1711 (2005)

[21] Gadre, A., Maczka, D., Spinello, D., McCarter, B., Stilwell, D., Neu, W., Roan, M., Hennage, J.: Cooperative localization of an acoustic source using towed hydrophone arrays. In: Proc. IEEE/OES Autonomous Underwater Vehicles, pp. 1 –8 (2008)

[22] Gilbertson, E., Reed, B., Leighton, J., Cheung, M., Hover, F.: Experiments in dynamic control of autonomous marine vehicles using acoustic modems. In: Proc. IEEE International Conf. on Robotics and Automation (2013)

[23] Heidemann, J., Stojanovic, M., Zorzi, M.: Underwater sensor networks: applications, advances and challenges. Philosophical Transactions of the Royal Society A: Mathematical, Physical and Engineering Sciences **370**(1958), 158–175 (2012)

[24] Julier, S., Uhlmann, J.: New extension of the Kalman filter to nonlinear systems. In: AeroSense'97, pp. 182–193. International Society for Optics and Photonics (1997)

[25] Leonard, N., Paley, D., Lekien, F., Sepulchre, R., Fratantoni, D., Davis, R.: Collective motion, sensor networks, and ocean sampling. Proc. IEEE **95**(1), 48 –74 (2007)

[26] Liao, E., Hollinger, G., Djugash, J., Singh, S.: Preliminary results in tracking mobile targets using range sensors from multiple robots. Distributed Autonomous Robotic Systems 7 pp. 125–134 (2006)

[27] Mostofi, Y., Chung, T., Murray, R., Burdick, J.: Communication and sensing trade-offs in decentralized mobile sensor networks: a cross-layer design approach. In: Proc. 4th International Symposium on Information Processing in Sensor Networks, p. 16. IEEE Press (2005)

[28] Rife, J., Rock, S.: Design and validation of a robotic control law for observation of deep-ocean jellyfish. IEEE Trans. Robotics **22**(2), 282 –291 (2006)

[29] Schneider, T., Schmidt, H.: Unified command and control for heterogeneous marine sensing networks. Journal of Field Robotics **27**(6), 876–889 (2010)

[30] Sinopoli, B., Schenato, L., Franceschetti, M., Poolla, K., Jordan, M., Sastry, S.: Kalman filtering with intermittent observations. IEEE Trans. Automatic Control **49**(9), 1453–1464 (2004)

[31] Skomal, G., Benz, G.: Ultrasonic tracking of greenland sharks, somniosus microcephalus, under arctic ice. Marine Biology **145**(3), 489–498 (2004)

[32] Soares, J., Aguiar, A., Pascoal, A., Martinoli, A.: Joint ASV/AUV range-based formation control: Theory and experimental results. In: Proc. International Conf. Robotics and Automation (ICRA) (2013)

[33] Takasu, T., Yasuda, A.: Development of the low-cost RTK-GPS receiver with an open source program package RTKLIB. In: International Symposium on GPS/GNSS, International Convention Center Jeju, Korea (2009)

[34] Vázquez-Rowe, I., Iribarren, D., Moreira, M.T., Feijoo, G.: Combined application of life cycle assessment and data envelopment analysis as a methodological approach for the assessment of fisheries. The International Journal of Life Cycle Assessment **15**(3), 272–283 (2010)

[35] Vidal, R., Shakernia, O., Kim, H., Shim, D., Sastry, S.: Probabilistic pursuit-evasion games: theory, implementation, and experimental evaluation. IEEE Trans. Robotics and Automation **18**(5), 662 – 669 (2002)

[36] Voegeli, F., Smale, M., Webber, D., Andrade, Y., O'Dor, R.: Ultrasonic telemetry, tracking and automated monitoring technology for sharks. Environmental Biology of Fishes **60**(1), 267–282 (2001)

[37] Zhou, K., Roumeliotis, S.: Optimal motion strategies for range-only constrained multisensor target tracking. IEEE Trans. Robotics **24**(5), 1168–1185 (2008)